JOURNAL OF CATALYSIS 53, 366–373 (1978)

Crystallite Size Effects during the Catalytic Oxidation of Propylene on $Pt/\gamma\text{-}Al_2O_3$

LUIS M. CARBALLO* AND EDUARDO E. WOLF

Department of Chemical Engineering, University of Notre Dame, Notre Dame, Indiana 46556

Received October 3, 1977; revised March 3, 1978

This work reports results on the kinetics and crystallite size effects during the catalytic oxidation of propylene on $Pt/\gamma\text{-}Al_2O_3$. The experiments were carried out in a reactor–chemisorption apparatus that can be used to study the reaction kinetics and *in situ* characterization of the catalyst by measuring the chemisorption of H_2. It was found that reaction rate decreased during reaction and that oxygen pretreatment restored the catalyst activity. Kinetic studies were carried out using catalysts with 1% Pt and average crystallite sizes of 11, 60, and 144 Å. The kinetic results revealed a complex dependence between reaction rate and C_3H_6 concentration. At low propylene concentration, the reaction rate increased with concentration until it reached a maximum. A further increase in reactant concentration produced a decrease in reaction rate, and at high reactant concentration the reaction rate became zero order. The reaction rates per unit mass of catalyst were quantitatively similar for catalysts with different crystallite sizes; consequently, the reaction rates per unit area of catalyst (specific reaction rates) were different since there was a tenfold difference in average crystallite size. The results indicated that the reaction exhibits demanding behavior and that the specific reaction rate increases significantly with crystallite size. This finding indicates that larger crystallites catalyze the oxidation of propylene more effectively which has also been observed in the case of CO oxidation on $Pt/\alpha\text{-}Al_2O_3$.

INTRODUCTION

The complete oxidation of hydrocarbons is a technologically important reaction in automobile pollution control. Propylene oxidation is the model reaction of hydrocarbon oxidation in catalytic converters. Several studies of the kinetics of this reaction have been published (1–4). However, the effect of crystallite size on the specific reaction rate which is relevant to determination of the structure sensitivity of this reaction has not been reported. Previous investigations in this Department by McCarthy *et al.* (*5*) on CO oxidation suggest a demanding behavior at low CO concentration and a facile behavior at high CO concentrations. Paralleling the studies of Huang and Carberry (*6*), we examined the effect of crystallite size on the specific activity of a $Pt/\gamma\text{-}Al_2O_3$ catalyst during propylene oxidation as well as the effect of catalyst pretreatment on catalyst activity.

Propylene oxidation has been studied in a number of metallic catalysts at various conditions (*1–4*). Patterson and Kemball (*1*) studied the oxidation of propylene on Pt films and reported a -0.2 reaction order with respect to C_3H_6 pressure and a 0.5 order with respect to oxygen pressure. Morooka and Ozaki (*2*) studied the kinetics of this reaction on 17 metal oxides, Pt, and Pd, all supported on silicon carbide. For Pt, using a power-law expression, these authors reported a -0.74 order in

* Present Address: Departamento de Ingenieria Quimica, Universidad Nacional, Bogota, Colombia.

0021-9517/78/0533-0366$02.00/0

C_3H_6 concentration and a 1.45 order in oxygen concentration. They also found that the larger the heat of formation of the oxides, the less active the catalyst. Cant and Hall (*7*) studied the oxidation of ethylene and propylene over silica-supported Pt, Pd, Ir, Ru, and Rh. The specific activity fell in the same order in which the catalysts are listed and correlated with percentage *d* character of the metals. The partial oxidation products were found to be acetaldehyde and acetic acid, with Pt producing mainly CO_2 and H_2O. These authors found that, on Pt, the total reaction rate decreased with olefin pressure and increased with oxygen pressure. Voltz *et al.* (*4*) studied the kinetics of CO and C_3H_6 oxidation in the presence of H_2O on a Pt–Al_2O_3 catalyst. These authors reported that the oxidation rates of CO and C_3H_6 increased with an increase in O_2 concentration and exhibited an adjusted bimolecular-type kinetics with respect to CO and C_3H_6. NO was found to inhibit the oxidation rates of both CO and C_3H_6.

The above studies indicate that the catalyst activity is influenced by surface interaction between O_2, C_3H_6, and other gases such as CO and NO. Nishiyama and Wise (*8*) reported that carbon contamination of the surface greatly reduced the rate of O_2 adsorption on Pt. Preadsorbed O_2 reacts readily with gaseous CO, but a very slow reaction was noted in the case of preadsorbed CO with O_2. Recent studies of elementary steps involved in catalytic oxidation clearly point out the need to consider the state of the surface prior to and during the reaction. Blakely and Somorjai (*9*) recently reported that high-Miller index Pt single-crystal surfaces are not stable in the presence of oxidizing atmospheres, and surface reconstruction occurs depending on the environment, the type of surface reconstruction being a function of the initial step density. These findings point out that crystallite size effects can occur during oxidation reactions. The objective of this work is to study crystallite size effects at different reactant concentrations and the effect of catalyst pretreatment on activity and deactivation.

EXPERIMENTAL METHODS

The apparatus used in this work has been described previously (*10*). It consists of an integrated reactor–chemisorption apparatus designed for reaction kinetic studies and *in situ* measurement of H_2 chemisorption by the pulse technique. A schematic diagram of the equipment is shown in Fig. 1. The apparatus consists of a section for metering and mixing the reactants and a quartz reactor (30 cm long, 1 cm i.d.) surrounded by an electrical heater with a temperature controller. The temperature is measured by a thermocouple contained in a thermowell positioned at the center of the catalyst bed. The gaseous reactants flow downward through the catalyst bed and the reaction products are analyzed at the reactor outlet. The analysis is carried out in a gas chromatograph (gc) using a 10-ft Porapak Q column with He as a carrier gas.

The reactor can be operated as a differential or recycle reactor. A bellows pump is used to recirculate the gaseous reactants when operating in recycle mode. All the

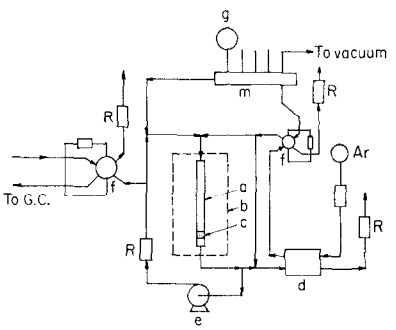

FIG. 1. Schematic diagram of the apparatus: (a) reactor, (b) electrical heater, (c) catalyst bed, (d) TC cell, (e) recirculation bellows pump, (f) gc sampling valve, (g) vacuum gage, (m) manifold, (R) rotameter, and (Ar) Argon cylinder.

experiments reported in this paper were carried out using the reactor as a differential reactor.

The apparatus can also be used to measure the chemisorption of H_2. This capability allows *in situ* characterization of the state of the metal during different stages of the kinetic studies. Hydrogen chemisorption was primarily used to estimate the average crystallite size. When the reactor is used as a chemisorption apparatus, ultrahigh-purity Argon is sent through the catalyst and through a thermal conductivity (TC) detector instead of through the gc. Pulses of H_2 diluted in Ar are injected into the carrier gas stream by means of a gc sampling valve (seven ports). The H_2 pulses are adsorbed by the catalyst until saturation occurs, in which case the fraction of H_2 not adsorbed is detected by the TC cell. A detailed examination of the experimental parameters involved in the H_2 chemisorption measurements has been recently carried out in our research group (*10*). The results indicate that high reproducibility can be obtained when the catalyst surface is properly preconditioned prior to the chemisorption experiments.

Catalyst. A 1% Pt/γ-Al_2O_3 catalyst was prepared by impregnation of γ-alumina (Harshaw, 192 m^2/g) with chloroplatinic acid. The catalyst preparation consisted of adding an aqueous solution containing the desired metal content to the alumina powder (200 mesh). The slurry is heated at 80°C while stirring continuously until all the water is evaporated. The catalyst is then dried overnight in air at 110°C and stored. The sample to be used (0.5–1 g) is weighed, placed in the reactor, dried again in Ar for 6 hr at 110°C, and then reduced in H_2 for 12 hr at 500°C. After reduction, the metal dispersion is estimated by H_2 chemisorption. The average crystallite size of the catalyst prepared by the above procedure was about 11 Å. Catalysts with larger crystallites were prepared by sintering the 11-Å catalyst in O_2 at 700°C for 10 and 30 hr, producing catalysts with 60- and 144-Å crystallites, respectively. After sintering in O_2, the catalysts were reduced again in H_2 at 500°C for 12 hr in order to obtain a reduced Pt surface.

Procedure. After the catalyst has been prepared and reduced, H_2 chemisorption measurements were carried out to determine the average crystallite size. A typical catalyst pretreatment used during H_2 chemisorption consisted of 12 hr of reduction in H_2 at 500°C, followed by 16 hr of degassing in Ar at 500°C and then cooling to room temperature in flowing Ar. The degassing period was necessary to clean the surface from H_2 used during reduction.

The kinetic experiments were carried out after catalyst characterization. It was found that reproducibility could be obtained only if the catalyst is pretreated in oxygen prior to each experiment. As discussed later, 2 hr of pretreatment in O_2 at 360°C gives the highest reaction rate and minimum deactivation. After O_2 pretreatment, the reactor was cooled to reaction temperature in flowing O_2. A stream of He, used as a diluent, was then introduced into the reactor, and the propylene feed was added to the He–O_2 mixture. After a stabilization period, the inlet and outlet concentrations and flow rates were measured. To avoid a temperature increase during reaction, the reactor was operated at a conversion lower than 20%. In accord with the low conversion level used, the reactor was considered to be a differential reactor and the rate was calculated as

$$r = (F_p/A_{Pt})x,$$

where r = specific rate (grams·moles per square meter·minutes); F_p = propylene flow rate (grams·moles per minute); A_{Pt} = platinum surface area (square meters); and x = propylene conversion.

The propylene concentrations were varied from 0.1 to 2% (v/v), whereas the oxygen

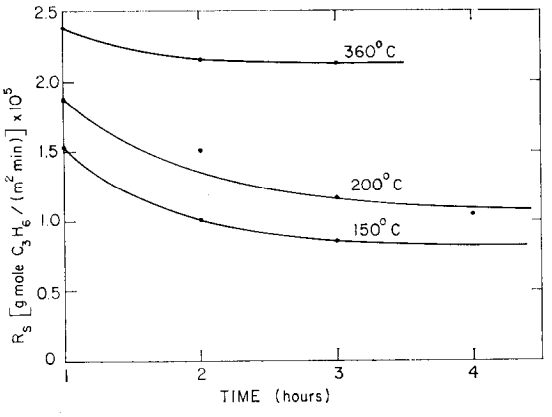

FIG. 2. Catalyst pretreatment at three different temperatures (d = 144 Å, T = 130°C). Specific rate vs time of reaction.

concentration remained a constant 20% (v/v). In one run, the oxygen concentration was varied to establish the effect of this variable on the reaction rate.

Two total flow rates (50 and 100 cm³/min) were used to test interparticle mass transfer effects. No effect of the flow rate on the reaction rate was observed, ruling out mass transfer limitations on the gas film; hence all experiments were carried out at a flow rate of 100 cm³/min. Using the calculations suggested by Carberry (*11*) no intraparticle mass transfer limitations were found to be important (see Appendix).

RESULTS

Preliminary experiments indicated that the rate of propylene oxidation decreased with time, suggesting that some type of catalyst poisoning was occurring (*12*). The catalyst activity was recovered by pretreating the catalyst in oxygen for 2 hr, prior to each experiment. However, we found that the initial activity was a function of the pretreatment temperature. Figure 2 shows the specific reaction rates (grams·moles per square meter·minutes) versus time for three different pretreatment temperatures. The catalyst used in the experiments reported in Fig. 2 has an average crystallite size of 144 Å, and the reaction temperature was 130°C. The results indicate that the catalyst activity increases and the deactivation rate decreases as the pretreatment temperature increases. In accord with the above results, a standard pretreatment of 2 hr in oxygen at 360°C was used prior to each run.

The reaction kinetics was determined at four temperatures (100, 110, 120, and 130°C) using catalysts with crystallite sizes of 11, 60, and 144 Å. The specific reaction rates (gram·moles of C_3H_6 per square meter·minutes) versus C_3H_6 concentrations are shown in Fig. 3 for the catalyst with an 11-Å average crystallite size. The results indicate that, at low C_3H_6, the reaction rate increases with C_3H_6 until it reaches a maximum. The rate then decreases and tends to be concentration independent at high C_3H_6 concentration. The data cannot be fitted to a kinetic model obtained from a simple reaction mechanism and suggest a complex reaction network. The kinetic results exhibit similar trends as a bimolecular Langmuir reaction, but attempts to obtain a good fit using such expressions were not successful.

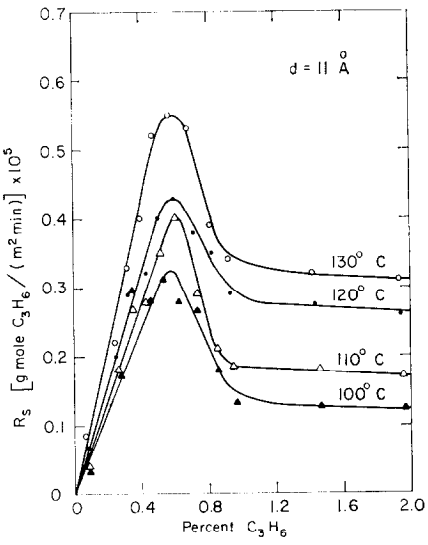

FIG. 3. Specific rate vs C_3H_6 concentration (d = 11 Å, four different temperatures).

The global reaction rates obtained at $T = 130°C$ for the catalyst with crystallite sizes of 11, 60, and 144 Å are plotted in Fig. 4 versus C_3H_6 concentration. Surprisingly, a tenfold increase in particle size does not change significantly the global rate, which slightly decreases as particle size increases. Consequently, when the global rates are converted to the specific rates shown in Fig. 5, a considerable difference in specific rates is obtained, with the catalyst of larger crystallite size (144 Å) exhibiting the higher specific rate. The results shown in Fig. 5 indicate that the specific reaction rate increases with crystallite size and that this effect is manifest throughout the entire concentration range used in this work. The results for other temperatures are summarized in Table 1 and follow the same trend as in Fig. 5.

The effect of oxygen concentration on the reaction rate is shown in Fig. 6 for a catalyst with $d = 11$ Å. The data were obtained at a fixed C_3H_6 concentration, at $T = 130°C$, varying the oxygen concentration. The order with respect to oxygen concentration is 0.5, which agrees with previous work (*1*).

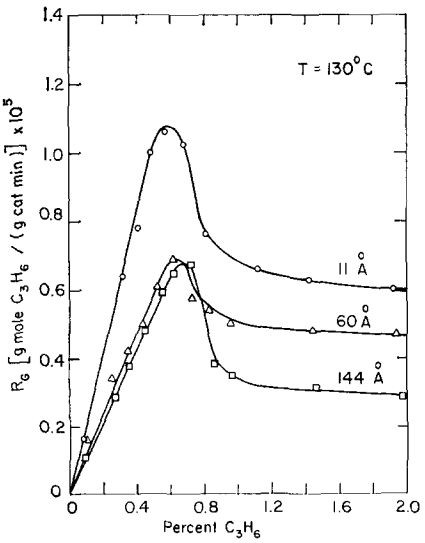

FIG. 4. Global reaction rate vs C_3H_6 concentration ($T = 130°C$, three different particle sizes).

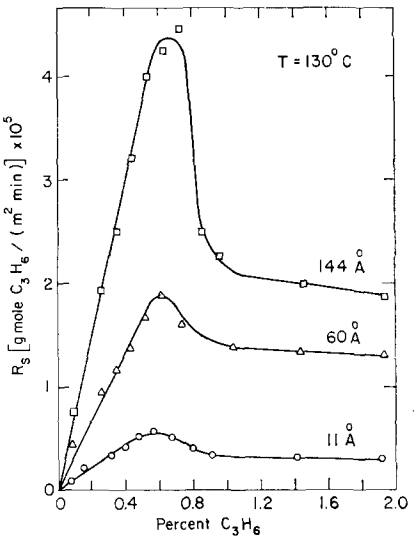

FIG. 5. Specific reaction rate vs C_3H_6 concentration ($T = 130°C$, three different particle sizes).

DISCUSSION

The most significant facts reported in this work are the effect of catalyst pretreatment, the reaction kinetics, and the effect of crystallite size on the specific activity.

The effect of catalyst pretreatment on catalyst activity and catalyst deactivation suggests a self-poisoning mechanism by formation of carbon residues (*12*). Thus oxygen pretreatment appears to burn off such residues, regenerating the surface. Increasing the pretreatment temperature would increase the rate of carbon burn-off thus producing a cleaner surface with higher activity. The oxygen pretreatment, however, can modify the surface composition. Hydrogen chemisorption measurements carried out after oxygen pretreatment at 360°C *without* reduction indicate a 68% reduction of the amount of H_2 chemisorbed relative to the amount of H_2 chemisorbed after reduction. On bulk Pt, gentle heating in air or oxygen to temperatures of about 400 to 500°C renders a thin film, probably of PtO_2 (*14*). This process could also be present in the case of our highly dispersed catalyst. Furthermore, the reaction takes place in an oxidizing

TABLE 1

Specific Rates (R_s) for Three Different Particle Sizes and Four Different Temperatures[a]

$\bar{d}_p$ (Å)	C_3H_6 (%)	100°C	C_3H_6 (%)	110°C	C_3H_6 (%)	120°C	C_3H_6 (%)	130°C
11 (1.93	0.092	0.032	0.091	0.038	0.084	0.066	0.080	0.084
m^2/g of catalyst)	0.26	0.176	0.256	0.184	0.252	0.203	0.248	0.218
	0.33	0.282	0.336	0.273	0.332	0.290	0.322	0.330
	0.436	0.271	0.434	0.282	0.425	0.318	0.405	0.402
	0.526	0.314	0.518	0.345	0.505	0.402	0.478	0.519
	0.634	0.282	0.606	0.400	0.598	0.430	0.570	0.550
	0.737	0.266	0.732	0.290	0.711	0.377	0.675	0.530
	0.858	0.178	0.850	0.212	0.818	0.348	0.808	0.392
	0.969	0.131	0.956	0.184	0.932	0.286	0.919	0.343
	1.47	0.129	1.46	0.176	1.43	0.276	1.42	0.324
	1.97	0.127	1.96	0.170	1.94	0.262	1.92	0.309
60 (0.362	0.095	0.103	0.094	0.133	0.088	0.263	0.080	0.452
m^2/g of catalyst)	0.276	0.542	0.275	0.556	0.275	0.573	0.259	0.926
	0.369	0.700	0.370	0.664	0.361	0.886	0.348	1.17
	0.458	0.932	0.454	1.028	0.452	1.09	0.440	1.37
	0.546	1.21	0.532	1.53	0.527	1.64	0.526	1.67
	0.648	1.15	0.634	1.48	0.631	1.56	0.616	1.898
	0.753	1.06	0.740	1.36	0.736	1.46	0.729	1.60
	0.872	0.640	0.846	1.22	0.839	1.37	0.834	1.50
	0.973	0.607	0.952	1.07	0.944	1.28	0.938	1.39
	1.48	0.452	1.46	0.926	1.45	1.17	1.44	1.33
	1.987	0.300	1.962	0.847	1.95	1.14	1.94	1.31
144 (0.153	0.092	0.414	0.091	0.489	0.088	0.650	0.086	0.746
m^2/g of catalyst)	0.282	0.962	0.277	1.24	0.273	1.46	0.264	1.93
	0.381	0.998	0.366	1.83	0.358	2.24	0.353	2.51
	0.475	1.36	0.454	2.45	0.448	2.81	0.44	3.21
	0.568	1.72	0.544	3.00	0.539	3.27	0.526	3.98
	0.671	1.555	0.648	2.81	0.629	3.80	0.620	4.25
	0.774	1.37	0.752	2.57	0.733	3.59	0.716	4.47
	0.877	1.24	0.872	1.51	0.86	2.13	0.853	2.50
	0.979	1.14	0.974	1.37	0.966	1.82	0.958	2.26
	1.48	1.02	1.477	1.24	1.47	1.40	1.46	2.00
	1.98	0.86	1.98	1.04	1.98	1.12	1.96	1.85

[a] $R_s \times 10^5$ g·mol of C_3H_6/m^2·min.

atmosphere which can also affect the metal surface composition. Pareja and co-workers (*16*) have shown that striking surface rearrangements take place during H_2 oxidation in the presence of traces of oxygen on Ni and Pt ribbons. These authors examined the catalyst surface with optical and scanning microscopes after and during exposure to the reaction mixture at 260°C. They observed that a gross surface rearrangement occurs during the reaction, whereas no change was observed when exposing catalyst to H_2–N_2 or pure H_2 at the same temperature and for long periods of time. It was found that, when changes occurred, some edges disappeared in favor of facets and that this effect increased with the O_2 concentration in the reaction mixture.

The kinetic results reported here can only be qualitatively compared with those reported in the literature due to the

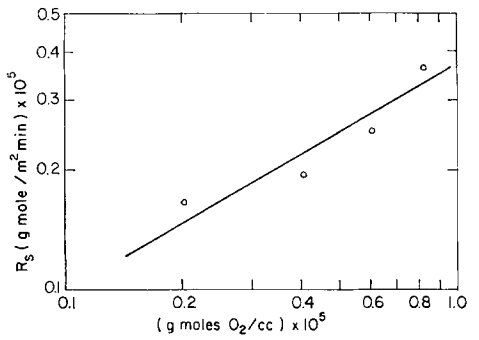

FIG. 6. Specific reaction rate vs oxygen concentration (d = 11 Å, T = 130°C, x_p = 0.01).

different type of pretreatment used in this work. Nonetheless, our data partially agree with the kinetics observed by other investigators in the corresponding concentration range. Voltz *et al.* (*4*) also describes a first-order behavior at low C_3H_6 concentration as was found in this work. At high C_3H_6 concentration, our data show negative- to zero-order behavior in accord with the results reported by Patterson and Kemball (*1*), Morooka and Ozaki (*2*), Cant and Hall (*7*), and Voltz *et al.* (*4*). However, our data do not fit a kinetic expression based on a simple reaction mechanism such as a bimolecular Langmuir–Hinshelwood kinetics. Thus our results suggest a complex reaction network in a manner similar to that in the investigation by Cant and Hall (*7*).

An apparent activation energy of about 10 kcal/mol can be calculated for a catalyst of 11-Å crystallite size by plotting the log of the reaction rate vs $1/T$. This value for the apparent activation energy is somewhat lower than values reported previously, which are in the range 15–20 kcal/mol. We believe that the lower activation energy obtained in this work is due to the different catalyst pretreatment used.

The most significant result obtained in this work is the increase in the specific reaction rate with increase in average crystallite size. Implicit in the previous statement is the assumption that, during sintering, the major path of area reduction is by crystallite growth instead of incapsulation of the metal by the support. Fiedorow and Wanke (*17*) and Ruckenstein and Malhotra (*18*) have demonstrated with electron micrographs that, in the temperature range used in this work, the major result of heating the catalyst in air is crystallite growth. MacIver *et al.* (*19*) reported that, when γ-alumina was heated for 24 hrs at 700°C, the reduction of the total area (BET) was about 12%. Similar results were obtained by Fiedorow and Wanke (*17*) in a study of the sintering of a Pt/Al_2O_3-supported catalyst. Furthermore, if sealing of the metal in the support would prevent H_2 chemisorption, as shown by our adsorption measurement, then it would surely prevent the reaction from occurring. Consequently, if sealing of the metal is a relevant mechanism of metal area reduction, then the specific reaction rate should decrease in proportion to the metal area instead of increasing as shown by our result. Therefore, our assumption that metal area reduction is accomplished by crystallite growth is well justified on the basis of independent evidence and our own results. Furthermore, McCarthy *et al.* (*5*) also reported that, during CO oxidation on Pt/α-Al_2O_3, the specific reaction rate also increased with crystallite size at low CO concentration. However, in our case, the demanding behavior (*15*) is manifest throughout the entire concentration range used, whereas during CO oxidation the reaction is demanding at low CO concentration and facile at high CO concentration. The metal crystallites can be envisioned by the truncated cubo octahedra model depicted by Bond (*13*), hence increasing crystallite size decreases the fraction of Pt atoms in edges and kinks and increases the fraction of atoms in terraces. If our results are interpreted in terms of the above model, it can be concluded that propylene is more readily oxidized in the crystallite terraces than in

kinks and edges. This suggests that the bonds between the metal and O_2 and propylene are less strong in the terraces, thus leading to higher specific rates.

It is significant though that at least in two instances of reactions involving oxidation of CO or C_3H_6 the same geometric effects are observed, namely, that the specific reaction rates increase with increasing crystallite size. Efforts are underway to determine if these effects are merely geometric as discussed in the previous paragraph or if they are also determined by the surface composition.

APPENDIX

Intraparticle Isothermal Diffusion

Intraparticle diffusion intrusions were estimated by calculating the following expressions, assuming first-order kinetic [Ref. (*11*), p. 223].

$$\eta\phi^2 = \frac{L^2 R_v}{D_{eff} C_0} \tag{1}$$

and

$$Bi_m = \frac{L k_g}{D_{eff}} \tag{2}$$

where η is the intraphase effectiveness factor, ϕ^2 is the square of the Thiele modulus; D_{eff}, is the effective diffusivity; and L is the particle diameter.

DATA

T = 130°C, d = 11 Å, $\%C_3H_6$ = 0.08
R = 3.3×10^{-8} g·mol/sec·cm³
C_0 = 2.42×10^{-8} g·mol/cm³
D_{eff} = 1.64×10^{-3} cm²/sec (calculated by accounting for ordinary diffusion of C_3H_6 in the He–O_2 mixture and Knudsen diffusion; the particle porosity used was 0.371 and the tortuosity was 2.1)
k_g = 2978 cm/sec
L = 0.0037 cm (200-mesh powder)

Substituting these values into Eqs. (1) and (2), we obtain $\eta\phi^2 = 0.0114$ and $Bi_m = 6.718$.

The above values confirm the absence of intraparticle diffusion which can be also verified by entering the values of $\eta\phi^2$ and Bi_m in Figs. 5–11 of Ref. (*11*) to obtain $\eta = 1$.

ACKNOWLEDGMENT

Thanks are due to the National Science Foundation for financial support under Grant 7600699.

REFERENCES

1. Patterson, W. R., and Kemball, C., *J. Catal.* **2**, 465 (1963).
2. Morooka, Y., and Ozaki, A., *J. Catal.* **5**, 116 (1966).
3. Cant, N. W., and Hall, W. K., *J. Catal.* **22**, 310 (1971).
4. Voltz, S. E., Morgan, C. R., Liederman, D., and Jacob, S., *Ind. Eng. Chem. Prod. Res. Develop.* **12**, 294 (1973).
5. McCarthy, E., Zahradnik, J., Kuczynski, G. C., and Carberry, J. J., *J. Catal.* **39**, 29 (1975).
6. Huang, T., and Carberry, J. J., Private communication.
7. Cant, N. W., and Hall, W. K., *J. Catal.* **16**, 220 (1970).
8. Nishiyama, Y., and Wise, H., *J. Catal.* **32**, 50 (1974).
9. Blakely, D. W., and Somorjai, G. A., *Surface Sci.* **65**, 453 (1977)
10. Serrano, C., Carballo, L., Wolf, E. E., and Carberry, J. J., *J. Catal.* **52**, 507 (1978).
11. Carberry, J. J., "Chemical and Catalytic Reaction Engineering." McGraw-Hill, New York, 1976.
12. Wolf, E. E., and Petersen, E. E., *J. Catal.* **46**, 190 (1977).
13. Bond, G. C., IV International Congress on Catalysis, Moscow, 1968, Preprint 67.
14. Chastin, J. C., *Platinum Metals Rev.* **19**, 135 (1975).
15. Boudart, M., *Advan. Catal.* **20**, 153 (1969).
16. Pareja, P., Amariglo, A., Piquard, G., and Amariglio, H., *J. Catal.* **46**, 225 (1977).
17. Fiedorow, R. M. J., and Wanke, S. E., *J. Catal.* **43**, 34 (1976).
18. Ruckenstein, E., and Malhotra, M. L., *J. Catal.* **41**, 303 (1976).
19. MacIver, D. S., Tobin, H. H., and Barth, R. T., *J. Catal.* **2**, 485 (1963).